Chapter 6

Prescribed-time adaptive control for DC-DC boost converters

6.1 Introduction

This chapter addresses the critical task of voltage regulation in DC-DC boost converters, considering their uncertain dynamics, varying input voltage, output load current, and inherent complexities. To maximize performance and ensure robustness under diverse operating conditions, control of power converters becomes crucial as power sources and electrical loads become more nonlinear and unpredictable. Motivated by these challenges, we propose an adaptation law-based prescribed-time control methodology for the DC-DC boost converter. The adaptive controller is designed to guarantee prescribed-time stability in sliding mode for closed-loop systems by utilizing prescribed-time state estimators. This approach offers a promising solution to achieve desired voltage regulation within a predetermined time frame, providing greater efficiency and robustness in the operation of DC-DC boost converters.

The main contributions of this chapter are as follows:

(i) We propose a novel control methodology for regulating the output voltage of DC-DC boost converters. The approach is based on adaptation laws and prescribed-time control techniques, which enable precise and efficient voltage regulation under varying operating conditions.

(ii) The proposed control strategy ensures stability and robustness in the presence of uncertain dynamics in DC-DC boost converters, using prescribed-time state estimators and adaptive controllers.

(iii) A key aspect of this chapter is the incorporation of a prescribed-time estimator with sliding mode control, allowing us to achieve robust voltage regulation within a pre-defined time frame.

6.1.1 DC-DC boost converter model

Figure 6.1 shows a boost converter circuit diagram. The averaged model of the DC-DC boost converter under continuous conduction mode is given as [115]

$$\begin{aligned} \dot{z}_1(t) &= -\left(1-u(t)\right)\frac{z_2(t)}{L} + \frac{V_{\text{in}}}{L} \\ \dot{z}_2(t) &= \left(1-u(t)\right)\frac{z_1(t)}{C} - \frac{\theta}{C}z_2(t) \end{aligned} \tag{6.1}$$

where $\theta = \frac{1}{R_o}$, and state variables $z_1(t)$ and $z_2(t)$ denotes the average inductor current i_L, and the average capacitor voltage V_0 respectively. The components L, C, and R_0 represent the inductors, capacitors, and load resistors. The external input voltage V_{in} and the load resistance R_0 are unknown at this point. The duty ratio function is the control input $u(t)$ to the converter.

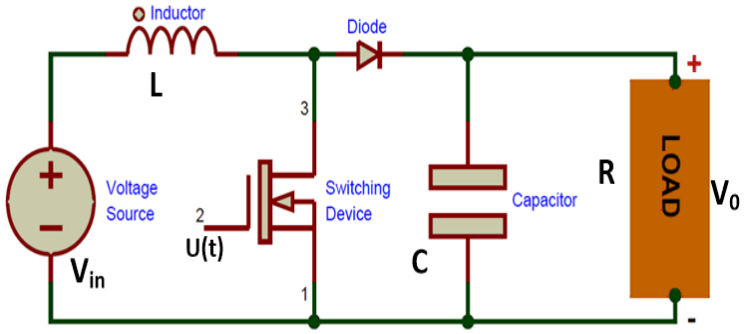

Figure 6.1: Circuit diagram of DC-DC boost converter.

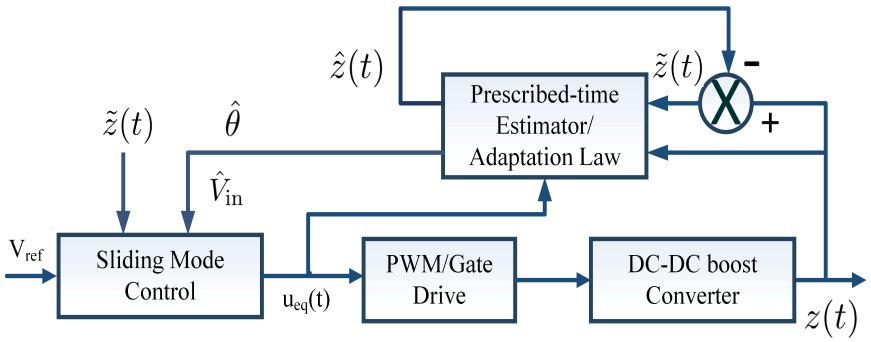

Figure 6.2: Schematic block diagram of the proposed prescribed-time adaptive state estimator-based sliding mode control for DC-DC boost converters.

6.2 Main results

The performance of the DC-DC boost converters is primarily measured by convergence time. Since the estimated parameter tracks its real value more rapidly and the estimation error is reduced in the finite-time period, the shorter convergence time is crucial for controlling power electronics converters. As a result, the convergence speed is improved in this part using an adaptive prescribed-time estimator. Then, a thorough justification is given to ensure that the parameter estimate error converges to zero within the given period t_p, which the users establish as a priori and independent of the starting error. The schematic block diagram of the proposed prescribed-time adaptive state estimator-based sliding mode control for DC-DC boost converters is illustrated in Figure 6.2.

6.2.1 Adaptive estimator-based SMC design

Thus, to realize the switched-gain scheme, there are two cases to be considered

1. $t < t_p$, i.e., before the prescribed-time;

2. $t \geq t_p$, i.e., after the prescribed-time;

Case 1. When $t < t_p$, for the boost converter system (6.1). Let us assume that state variables $z_1(t)$ and $z_2(t)$ are accessible. However, a prescribed-time state estimator is taken into account to facilitate the design of parameter adaptation laws for $\hat{\theta}$ and $\hat{V}_{\text{in}}$, the estimates of θ and V_{in}, respectively, which are unknown. In the follow-up, it will be demonstrated that $\hat{\theta} \to (1/R_o)$ and $\hat{V}_{\text{in}} \to V_{\text{in}}$ in a user defined time i.e. prescribed-time t_p. To this end, the following prescribed-time estimator is designed to estimate the load variation θ and input variation V_{in}

$$\begin{aligned} \dot{\hat{z}}_1(t) &= -(1-u)\frac{\hat{z}_2(t)}{L} + \frac{\hat{V}_{\text{in}}}{L} + K_1(t,t_p)\left(z_1(t) - \hat{z}_1(t)\right) \\ \dot{\hat{z}}_2(t) &= (1-u)\frac{\hat{z}_1(t)}{C} - \frac{\hat{\theta}}{C}z_2(t) + K_2(t,t_p)\left(z_2(t) - \hat{z}_2(t)\right) \end{aligned} \tag{6.2}$$

where $\hat{z}_1(t)$ and $\hat{z}_2(t)$ are the estimates of $z_1(t)$ and $z_2(t)$ respectively. $K_1(t,t_p)$ and $K_2(t,t_p)$ are the estimator gain relates prescribed-time t_p, which will be designed later.

Let $\tilde{z}_1(t) = z_1(t) - \hat{z}_1(t)$, $\tilde{z}_2(t) = z_2(t) - \hat{z}_2(t), \tilde{\theta} = \theta - \hat{\theta}$, and $\tilde{V}_{\text{in}} = V_{\text{in}} - \hat{V}_{\text{in}}$.

Now, subtracting (6.2) from (6.1), the dynamics of the state estimation error $\tilde{z}(t) = \hat{z}(t) - z(t)$ can be obtained as

$$\begin{aligned} \dot{\tilde{z}}_1(t) &= -(1-u(t))\frac{\tilde{z}_2(t)}{L} + \frac{\tilde{V}_{\text{in}}}{L} - K_1(t,t_p)\tilde{z}_1(t) \\ \dot{\tilde{z}}_2(t) &= (1-u(t))\frac{\tilde{z}_1(t)}{C} - \frac{\tilde{\theta}}{C}z_2(t) - K_2(t,t_p)\tilde{z}_2(t) \end{aligned} \tag{6.3}$$

The estimator gains related to prescribed-time t_p are designed as

$$\begin{aligned} K_1(t,t_p) &= \frac{K_{p1}}{(t_p-t)} \\ K_2(t,t_p) &= \frac{K_{p2}}{(t_p-t)} \end{aligned} \tag{6.4}$$

where K_{p1} and K_{p1} are the positive constants to be designed.

The adaptive laws for the estimation of θ and V_{in} is designed as

$$\begin{aligned} \dot{\hat{\theta}} &= -\gamma_1 z_2(t)\tilde{z}_2(t) \\ \dot{\hat{V}}_{\text{in}} &= \gamma_2 \tilde{z}_1(t) \end{aligned} \tag{6.5}$$

where $\gamma_1 > 0$ and $\gamma_2 > 0$ are design parameters.

Theorem 6.1 *When $t < t_p$, for the DC-DC boost converter system* (6.1)*, consider the adaptation law based prescribed-time state estimator* (6.3) *with the estimator gains in* (6.4) *and the adaptive laws for the estimation of θ and V_{in} in* (6.5)*. Then, the states estimation error $\tilde{z}_1(t)$ and $\tilde{z}_2(t)$ converge to zero, during the given period t_p.*

Proof. Consider the following quadratic Lyapunov candidate function:

$$V(t) = V_1(t) + V_2(t) \tag{6.6}$$

where $V_1(t)$ and $V_2(t)$ are defined as

$$\begin{aligned} V_1(t) &= \frac{1}{2}L\tilde{z}_1^2(t) + \frac{1}{2}C\tilde{z}_2^2(t) \\ V_2(t) &= \frac{1}{2\gamma_1}\tilde{\theta}^2 + \frac{1}{2\gamma_2}\tilde{V}_{\text{in}} \end{aligned}$$

Taking the time derivative of (6.6) along the solutions of (6.3) is

$$\begin{aligned} \dot{V}(t) =& -K_1(t,t_p)L\tilde{z}_1^2(t) - K_2(t,t_p)C\tilde{z}_2^2(t) - \tilde{\theta}\Big[z_2(t)\tilde{z}_2(t) \\ &+ \frac{1}{\gamma_1}\dot{\hat{\theta}}\Big] + \tilde{V}_{\text{in}}\left[\tilde{z}_1(t) - \frac{1}{\gamma_2}\dot{\hat{V}}_{\text{in}}\right] \end{aligned} \tag{6.7}$$

With the adaptation law (6.5), we now have

$$\dot{V}(t) = -\frac{K_{p1}}{(t_p-t)}L\tilde{z}_1^2(t) - \frac{K_{p2}}{(t_p-t)}C\tilde{z}_2^2(t)$$

Which can be further written as

$$\dot{V}(t) \leq -\gamma\frac{V_1(t)}{(t_p-t)} \tag{6.8}$$

where $\gamma = 2\min\{K_{p1}, K_{p2}\}$ From (6.8) and Lemma 4.4, one can get that $\tilde{z}_1(t)$ and $\tilde{z}_2(t)$ are bounded for all $t \in [0, t_p)$ and $\lim_{t\to t_p^-} V_1(t) = 0$, from which we can conclude that $\tilde{z}_1(t) \to 0$

and $\tilde{z}_2(t) \to 0$ in prescribed-time t_p. Which further implies that $\hat{z}_1(t) \to z_1(t)$ and $\hat{z}_2(t) \to z_2(t)$ in prescribed-time t_p.

Next, utilizing the above proposed prescribed-time estimator, the sliding surface is designed for voltage regulation in the prescribed time. To do so, we take into account the following switching surface:

$$s = \hat{z}_1(t) - \frac{V_{\text{ref}}^2}{\hat{V}_{\text{in}}}\hat{\theta} \tag{6.9}$$

where V_{ref} denotes the reference voltage. Differentiating the switching surface s with regard to time

$$\dot{s} = \dot{\hat{z}}_1(t) + \frac{V_{\text{ref}}^2}{\hat{V}_{\text{in}}}\dot{\hat{\theta}} - \frac{V_{\text{ref}}^2}{\hat{V}_{\text{in}}^2}\hat{\theta}\dot{\hat{V}}_{\text{in}} \tag{6.10}$$

Using (6.2), and (6.5), we further obtain

$$\begin{aligned}\dot{s} =& -(1-u(t))\frac{\hat{z}_2(t)}{L} + \frac{\hat{V}_{\text{in}}}{L} + K_1(t,t_p)\left(z_1(t) - \hat{z}_1(t)\right) \\ & - \gamma_1 \frac{V_{\text{ref}}^2}{\hat{V}_{\text{in}}} z_2(t)\tilde{z}_2(t) - \gamma_2 \frac{V_{\text{ref}}^2}{\hat{V}_{\text{in}}^2}\hat{\theta}\tilde{z}_1(t)\end{aligned} \tag{6.11}$$

Next, the equivalent control is obtained using the invariance condition and setting $\dot{s} = 0$

$$\begin{aligned}u_{\text{eq}}(t) =& 1 - \frac{1}{\hat{z}_2(t)}\left(\hat{V}_{\text{in}} + K_1(t,t_p)L\tilde{z}_1(t)\right) \\ & - \frac{L}{\hat{z}_2(t)}\left(\gamma_1 \frac{V_{\text{ref}}^2}{\hat{V}_{\text{in}}} z_2(t)\tilde{z}_2(t) + \gamma_2 \frac{V_{\text{ref}}^2}{\hat{V}_{\text{in}}^2}\hat{\theta}\tilde{z}_1(t)\right)\end{aligned} \tag{6.12}$$

where $\hat{z}_2(t)(0) > 0$, $\hat{V}_{\text{in}}(0) > 0$ and $u_{\text{eq}}(t)$ is the equivalent control. Further, utilizing (6.12) we propose the following prescribed time sliding mode control law which also satisfies the sliding condition

$$\begin{aligned}u(t) =& 1 - \frac{1}{\hat{z}_2(t)}\left(\hat{V}_{\text{in}} + K_1(t,t_p)L\tilde{z}_1(t)\right) \\ & - \frac{L}{\hat{z}_2(t)}\left(\gamma_1 \frac{V_{\text{ref}}^2}{\hat{V}_{\text{in}}} z_2(t)\tilde{z}_2(t) + \gamma_2 \frac{V_{\text{ref}}^2}{\hat{V}_{\text{in}}^2}\hat{\theta}\tilde{z}_1(t)\right) - \gamma_3 \frac{s}{(t_p - t)}\end{aligned} \tag{6.13}$$

where γ_3 is a small positive design constant. Using the designed control law (6.13), (6.11) can be further written as $\dot{s} = -\gamma_3 \frac{s}{(t_p-t)L}\hat{z}_2(t)$. Which further implies $s\dot{s} = -\gamma_3 \frac{s^2}{(t_p-t)L}\hat{z}_2(t) < 0$. Hence, the proposed prescribed-time state observer-based control law (6.13) guarantees the satisfaction of sliding mode condition $s\dot{s} \leq 0$. Moreover γ_3, L and $\hat{z}_2(t)$ are considered positive then one can ensure that s convergence to zero in prescribed-time t_p. ■

Case 2. When $t \geq t_p$, certain approximation errors continue to persist in the estimation of θ and V_{in}. It might cause a discrepancy between the estimated and real values of θ and V_{in}. Therefore, in order to remove the aforementioned error, an estimator is required.

The following estimator is taken into account in this regard:

$$\begin{aligned}\dot{\hat{z}}_1(t) &= -(1-u(t))\frac{\hat{z}_2(t)}{L} + \frac{\hat{V}_{\text{in}}}{L} + K_1\left(z_1(t) - \hat{z}_1(t)\right)\\ \dot{\hat{z}}_2(t) &= (1-u(t))\frac{\hat{z}_1(t)}{C} - \frac{\hat{\theta}}{C}z_2(t) + K_2\left(z_2(t) - \hat{z}_2(t)\right)\end{aligned} \tag{6.14}$$

where $K_1 > 0$ and $K_2 > 0$ are the observer gains.

Subtracting (6.14) from (6.1), the dynamics of the state estimation error $\tilde{z}(t) = \hat{z}(t) - z(t)$ can be obtained as

$$\begin{aligned}\dot{\tilde{z}}_1(t) &= -(1-u(t))\frac{\tilde{z}_2(t)}{L} + \frac{\tilde{V}_{\text{in}}}{L} - K_1\tilde{z}_1(t)\\ \dot{\tilde{z}}_2(t) &= (1-u(t))\frac{\tilde{z}_1(t)}{C} - \frac{\tilde{\theta}}{C}z_2(t) - K_2\tilde{z}_2(t)\end{aligned} \tag{6.15}$$

Theorem 6.2 *When $t \geq t_p$, for the DC-DC boost converter system* (6.1)*, consider the adaptation law-based estimator* (6.15) *and the adaptive law* (6.5)*. Then the states estimation error $\tilde{z}_1(t)$ and $\tilde{z}_2(t)$ eventually converge to zero in the presence of approximation error and remain zero for all future time.*

Proof. Taking the time derivative of (6.6) along the solutions of (6.15) results

$$\begin{aligned}\dot{V}(t) =& -K_1L\tilde{z}_1^2(t) - K_2C\tilde{z}_2^2(t) - \tilde{\theta}\left[z_2(t)\tilde{z}_2(t) + \frac{1}{\gamma_1}\dot{\hat{\theta}}\right]\\ &+ \tilde{V}_{\text{in}}\left[\tilde{z}_1(t) - \frac{1}{\gamma_2}\dot{\hat{V}}_{\text{in}}\right]\end{aligned} \tag{6.16}$$

Using the adaptation law (6.5) give us $\dot{V}(t) = -K_1L\tilde{z}_1^2(t) - K_2C\tilde{z}_2^2(t)$. Hence, utilizing the Lasalle's invariant principle [105] one can say that $\tilde{z}_1(t) \to 0$ and $\tilde{z}_2(t) \to 0$ asymptotically which further guarantee $\hat{z}_1(t) \to z_1(t)$ and $\hat{z}_2(t) \to z_2(t)$ asymptotically in presence of any approximation error. Next, in order to maintain the reference tracking beyond the terminal time, i.e. $t \geq t_p$, we consider the sliding surface (6.9). Further taking the time derivative of (6.9) we get

$$\dot{s} = \dot{\hat{z}}_1(t) + \frac{V_{\text{ref}}^2}{\hat{V}_{\text{in}}}\dot{\hat{\theta}} - \frac{V_{\text{ref}}^2}{\hat{V}_{\text{in}}^2}\hat{\theta}\dot{\hat{V}}_{\text{in}} \tag{6.17}$$

Now, substituting (6.5) and (6.9) into (6.17) results in

$$\begin{aligned}\dot{s} =& -(1-u(t))\frac{\hat{z}_2(t)}{L} + \frac{\hat{V}_{\text{in}}}{L} + K_1\left(z_1(t) - \hat{z}_1(t)\right)\\ &- \gamma_1\frac{V_{\text{ref}}^2}{\hat{V}_{\text{in}}}z_2(t)\tilde{z}_2(t) - \gamma_2\frac{V_{\text{ref}}^2}{\hat{V}_{\text{in}}^2}\hat{\theta}\tilde{z}_1(t)\end{aligned} \tag{6.18}$$

Further setting $\dot{s} = 0$, we obtain the equivalent control u_{eq} as

$$\begin{aligned}u_{\text{eq}}(t) =& 1 - \frac{1}{\hat{z}_2(t)}\left(\hat{V}_{\text{in}} + K_1L\tilde{z}_1(t)\right)\\ &- \frac{L}{\hat{z}_2(t)}\left(\gamma_1\frac{V_{\text{ref}}^2}{\hat{V}_{\text{in}}}z_2(t)\tilde{z}_2(t) + \gamma_2\frac{V_{\text{ref}}^2}{\hat{V}_{\text{in}}^2}\hat{\theta}\tilde{z}_1(t)\right)\end{aligned} \tag{6.19}$$

where $\hat{z}_2(t)(0) > 0$, $\hat{V}_{\text{in}}(0) > 0$ and u_{eq} is the equivalent control. Further, utilizing (6.19) we propose the following control law, which also satisfies the sliding condition

$$u(t) = u_{\text{eq}}(t) - \gamma_4 s \tag{6.20}$$

Substituting the equivalent control (6.19) into (6.20), we get

$$\begin{aligned} u(t) =& 1 - \frac{1}{\hat{z}_2(t)}\left(\hat{V}_{\text{in}} + K_1 L \tilde{z}_1(t)\right) \\ & - \frac{L}{\hat{z}_2(t)}\left(\gamma_1 \frac{V_{\text{ref}}^2}{\hat{V}_{\text{in}}} z_2(t)\tilde{z}_2(t) + \gamma_2 \frac{V_{\text{ref}}^2}{\hat{V}_{\text{in}}^2}\hat{\theta}\tilde{z}_1(t)\right) - \gamma_4 s \end{aligned} \tag{6.21}$$

where γ_4 is a small positive design constant. Using the designed control law (6.21), (6.11) can be further written as $\dot{s} = -\gamma_4 \frac{s}{L}\hat{z}_2(t)$. Therefore $s\dot{s} = -\gamma_4 \frac{s^2}{L}\hat{z}_2(t)$. Hence, the proposed state estimator-based sliding mode control law (6.21) guarantees the satisfaction of sliding mode condition $s\dot{s} \leq 0$. Moreover, γ_4, L and $\hat{z}_2(t)$ are considered positive, then one can ensure that s convergence to zero asymptotically and remains zero for all future time, i.e., $t \geq t_p$. ■

Remark 6.3 *Since the convergence time and estimation accuracy are known to be inversely correlated, increasing the convergence time will certainly result in a decrease in steady-state accuracy [116]. Since the majority of the time the system is operating in a steady state, it is imperative to ensure both steady-state accuracy and convergence time. Therefore, a switched-gain system is suggested to accomplish this purpose, although the timing of the transition in the gains is a crucial design consideration [113].*

6.2.2 Convergence analysis

Combining both cases one can say that for all $t \geq t_p$ we have $\tilde{z}_1(t) = \tilde{z}_2(t) = 0$ which further leads to $\tilde{V}_{\text{in}} = 0$ and $\hat{V}_{\text{in}} = V_{\text{in}}$. Further, the proposed control law (6.13)-(6.21) ensures the prescribed-time convergence of the sliding surface s. Hence, utilizing (6.9) we have $\hat{z}_1(t) = \frac{V_{\text{ref}}^2}{\hat{V}_{\text{in}}}\hat{\theta}$.

Furthermore, with the aid (6.2), we have

$$\dot{\hat{z}}_2(t) = (1 - u(t))\frac{\hat{z}_1(t)}{C} - \frac{\hat{\theta}}{C} z_2(t) + K_2(t, t_p)\left(z_2(t) - \hat{z}_2(t)\right) \tag{6.22}$$

Next, substituting the proposed prescribed-time control (6.13) in (6.22), we get

$$\begin{aligned} \dot{\hat{z}}_2(t) =& \frac{\hat{z}_1(t)}{C\hat{z}_2(t)}\left(\hat{V}_{\text{in}} + K_1(t, t_p) L \tilde{z}_1(t)\right) \\ & + \frac{L\hat{z}_1(t)}{C\hat{z}_2(t)}\left(\gamma_1 \frac{V_{\text{ref}}^2}{\hat{V}_{\text{in}}} z_2(t)\tilde{z}_2(t) + \gamma_2 \frac{V_{\text{ref}}^2}{\hat{V}_{\text{in}}^2}\hat{\theta}\tilde{z}_1(t)\right) \\ & + \gamma_3 \frac{s\hat{z}_1(t)}{C(t_p - t)} - \frac{\hat{\theta}}{C} z_2(t) + K_2(t, t_p)\tilde{z}_2(t) \end{aligned} \tag{6.23}$$

Further substituting $z_2(t) = \hat{z}_2(t) + \tilde{z}_2(t)$ and $\hat{z}_1(t) = \frac{V_{\text{ref}}^2}{\hat{V}_{\text{in}}}\hat{\theta}$ in the sliding mode yields the following:

$$\begin{aligned}\hat{z}_2(t)\dot{\hat{z}}_2(t) =& \frac{1}{C}\big(\hat{V}_{\text{in}} + K_1(t,t_p)L\tilde{z}_1(t)\big)\frac{V_{\text{ref}}^2}{\hat{V}_{\text{in}}}\hat{\theta} \\ &+ \frac{L}{C}\left(\gamma_1\frac{V_{\text{ref}}^2}{\hat{V}_{\text{in}}}z_2(t)\tilde{z}_2(t) + \gamma_2\frac{V_{\text{ref}}^2}{\hat{V}_{\text{in}}^2}\hat{\theta}\tilde{z}_1(t)\right)\frac{V_{\text{ref}}^2}{\hat{V}_{\text{in}}}\hat{\theta} \\ &- \frac{\hat{\theta}}{C}\big(\hat{z}_2(t) + \tilde{z}_2(t)\big)\hat{z}_2(t) + K_2(t,t_p)\tilde{z}_2(t)\hat{z}_2(t) \end{aligned} \tag{6.24}$$

After some simplification (6.24) can be written as

$$\begin{aligned}\frac{d\hat{z}_2^2(t)}{dt} =& \frac{2\hat{\theta}}{C}[V_{\text{ref}} - \hat{z}_2^2(t)] + \tilde{z}_1(t)\Bigg[K_1(t,t_p)L \\ &+ \gamma_2\hat{\theta}\frac{LV_{\text{ref}}^2}{\hat{V}_{\text{in}}^2}\Bigg]\frac{2V_{\text{ref}}^2}{C\hat{V}_{\text{in}}}\hat{\theta} + 2\Bigg[\gamma_1\hat{\theta}z_2(t)\frac{LV_{\text{ref}}^4}{C\hat{V}_{\text{in}}^2} \\ &- \hat{\theta}\frac{\hat{z}_2(t)}{C} + K_2(t,t_p)\hat{z}_2(t)\Bigg]\tilde{z}_2(t) \end{aligned} \tag{6.25}$$

Since, $\tilde{z}_1(t)$ and $\tilde{z}_2(t)$ converges to zero in prescribed-time t_p, then (6.25) reduced to $\frac{d\hat{z}_2^2(t)}{dt} = \frac{2\hat{\theta}}{C}[V_{\text{ref}} - \hat{z}_2^2(t)]$. Hence, observing (6.25) one can say that $\hat{z}_2(t)$ converges to true value in prescribed-time t_p and it can attains two values i.e. $\hat{z}_2(t) = V_{\text{ref}}$ and $\hat{z}_2(t) = -V_{\text{ref}}$. Because of (6.11), the existence of the sliding-mode only guaranteed when $\hat{z}_2(t) > 0$. Consequently, $\hat{z}_2(t)$ and $z_2(t)$ converges in prescribed-time to V_{ref}. Furthermore, utilizing (6.5), we get $\tilde{\theta} \to 0$. Finally, $\hat{\theta} \to (1/R_o)$ and $z_1(t) \to I_{\text{ref}}$.

Remark 6.4 *In order to obtain the prescribed-time convergence, we must ensure that $\tilde{z}_1(t)$ and $\tilde{z}_2(t)$ converge to zero first. Consequently, the estimator gains K_{p1}, K_{p2}, K_1, and K_2 should be chosen to be significantly bigger than the controller gain.*

6.3 Simulation and experiment results

A DC-DC boost converter with the following specifications: $V_{\text{in}} = 30\text{V}$, $R = 50\Omega$, $L = 564\mu\text{H}$, $C = 250\mu\text{F}$, $V_{\text{ref}} = 50\text{V}$ is utilized for the simulations and experiments. The MATLAB/Simulink interface is used to control and acquire data with the dSPACE MicroLabBox. The setup of the hardware available in the laboratory is shown in Figure 6.3. We evaluate the designed controller's performance under two courses of action: (1) output voltage regulation with variable input voltage and (2) output voltage regulation with variable load. The design parameters for the proposed control law (6.13)-(6.21) are $K_{p1} = 25$, $K_{p2} = 20$, $K_1 = 1560$, $K_2 = 1250$, $\gamma_1 = 5$, $\gamma_2 = 250$, $\gamma_3 = 0.3$, $\gamma_4 = 0.4$, and $t_p = 0.02s$.

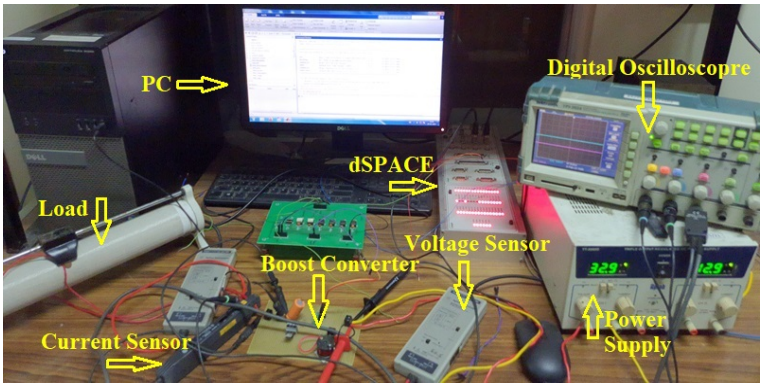

Figure 6.3: Experimental setup of the DC-DC boost converter.

Firstly through simulation, the effectiveness of the proposed control law to track the desired reference voltage and resilience to line and load uncertainty is evaluated. When the desired reference output voltage is kept at 50-volt, variable input voltages are supplied to the boost converter. Starting with a 25-volt input, we raise it to a 36-volt level. The obtained simulation results are shown in Figure 6.4 while holding V_{ref} and R constant at 50-volt and 50Ω, respectively. The simulation result in Figure 6.4(a) shows that the proposed prescribed-time adaptive estimator-based SMC technique delivered the appropriate voltage regulation within a prescribed time i.e., $0.02s$. The response of the load current is shown in 6.4(b) and the corresponding sliding surface is depicted in Figure 6.4(c).

Next, the DC-DC boost converter is subjected to a change in load resistance while the output voltage is maintained at 50-volt by adjusting the loads. The 50Ω start-up load resistance is gradually increased to 100Ω. The obtained simulation results are shown in Figure 6.5 while holding V_{ref} and V_{in} constant at 50-volt and 30-volt, respectively. As depicted in Figure 6.5(a), one can say that the output voltage consistently follows the desired reference voltage, even when there are variations in the load resistance. The response of the load current is shown in Figure 6.5(b) and the corresponding sliding surface is depicted in Figure 6.5(c).

Furthermore, the effectiveness of the proposed control law in tracking the desired reference voltage and its resilience to line and load uncertainty are evaluated through experiments. The experimental outcomes of the DC-DC boost converter using the suggested method are shown in Figures 6.6-6.9. Figure 6.6 and 6.7 illustrates the response due to a step change in the input voltage V_{ref} from 25-volt to 36-volt and vice-versa, while keeping the load resistance and reference voltage at 50Ω and 50-volt, respectively. Additionally, the transient response of the DC-DC converter under load resistance changes in a stepwise fashion is presented in Figure 6.8-6.9. In this case, the load is changed from 50Ω to 100Ω and vice-versa, while the input voltage and reference voltage are kept constant at 25-volt and 50-volt, respectively.

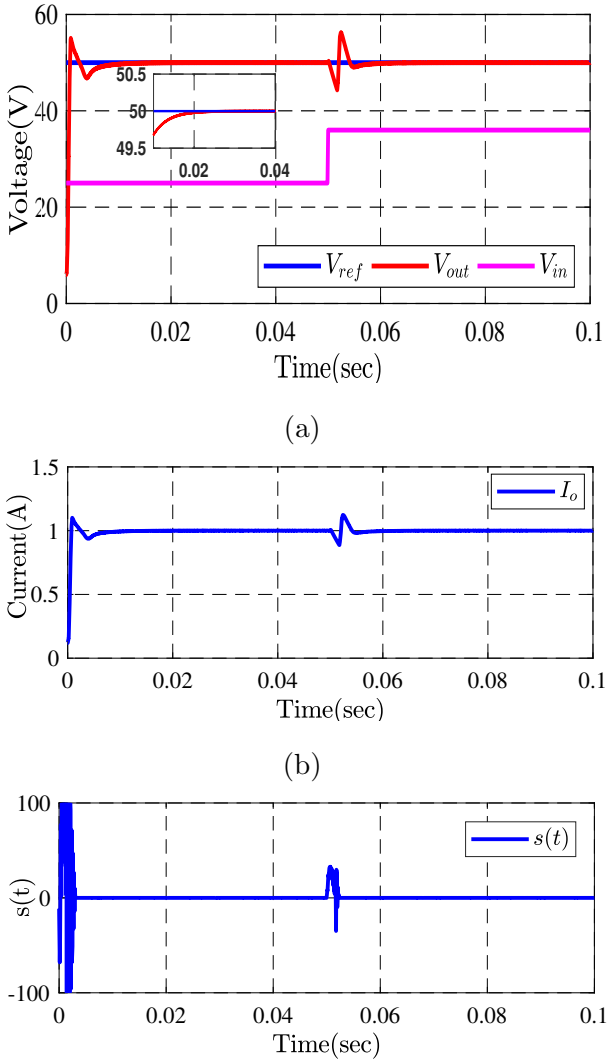

Figure 6.4: Simulation response: (a) varying input voltage; (b) corresponding load current; (c) corresponding sliding surface.

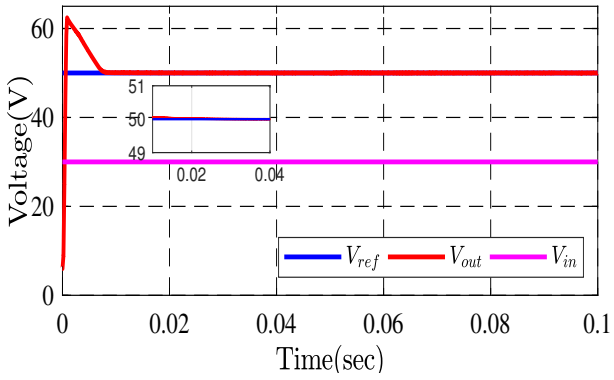

(a)

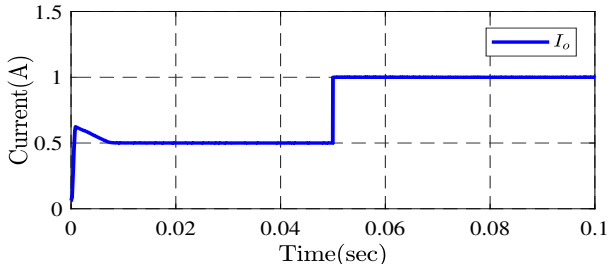

(b)

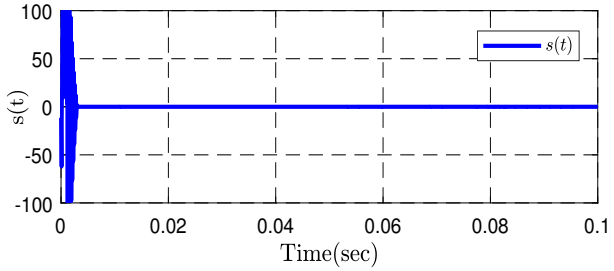

(c)

Figure 6.5: Simulation response: (a) varying output load; (b) corresponding load current; (c) corresponding sliding surface.

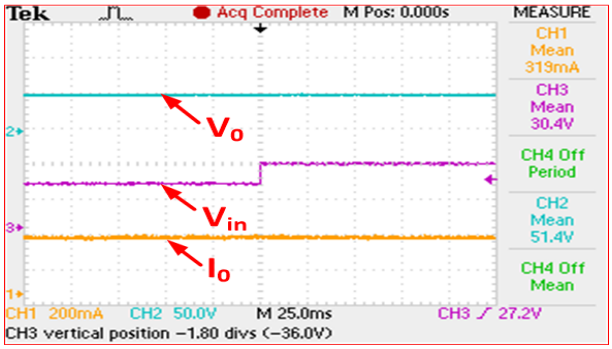

Figure 6.6: Experimental response varying input voltage from 25V to 36V.

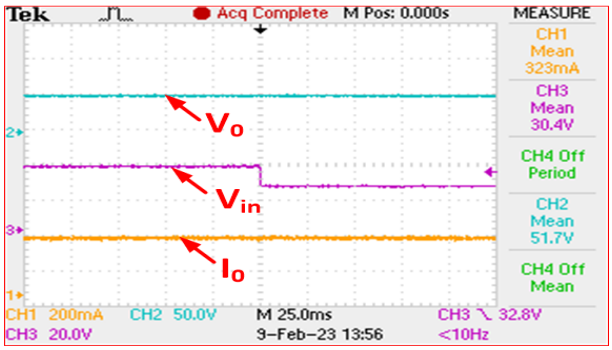

Figure 6.7: Experimental response varying input voltage from 36V to 25V.

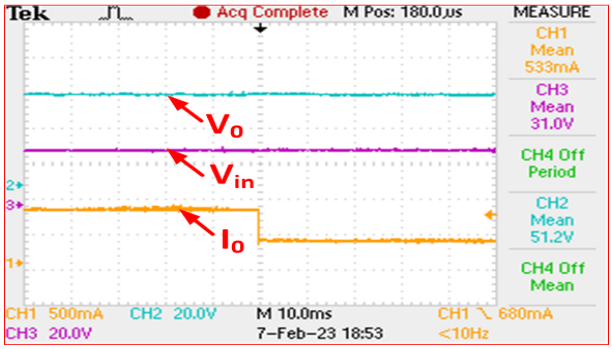

Figure 6.8: Experimental response varying load resistor from 50Ω to 100Ω.

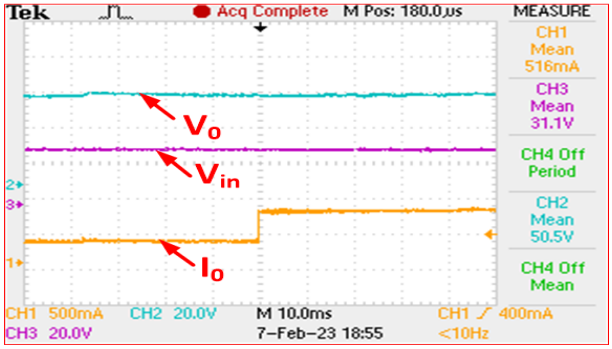

Figure 6.9: Experimental response varying load resistor from 100Ω to 50Ω.

The experimental results demonstrate the outstanding characteristics of the suggested prescribed-time adaptive estimator-based sliding-mode control in terms of its ability to handle the uncertain and fluctuating input voltage and output load, as evidenced by its robustness and recovery capability.

Remark 6.5 *It is worth noting that the control methods proposed in the existing literature lack the capability to fulfill user-defined performance requirements. In [118], the authors achieved the desired voltage tracking by proposing a robust nonlinear adaptive control employing an algebraic parameter identification technique. However, the convergence to the desired voltage is asymptotic. Additionally, the finite-time adaptive neural network observer-based approach in [119] provides finite-time voltage tracking, contingent on initial conditions. In contrast to existing approach, our designed control strategy ensures desired voltage tracking within a user-defined time, facilitating the attainment of specified performance in line with the designer's requirements. This underscores the capability of our control approach to meet user-defined performance requirements, providing precise and reliable control of convergence time—an advantageous feature in various applications.*

6.4 Conclusion

This chapter illustrated a prescribed-time adaptive estimator-based robust control strategy for the DC-DC boost converter under load resistance and input voltage fluctuation. In particular, we employed the adaptive law-based prescribed-time state estimator and sliding-mode control to obtain the prescribed time converge. Through extensive theoretical analysis, it is proven that the proposed scheme can ensure the regulation of desired voltage tracking within a prescribed time, which is a noteworthy feature of the proposed control. In the end, to testify the superiority of the designed control scheme, the simulations and experiments are performed for the following course of action: (i) varying the input voltage; (ii) varying the load resistance. In both the the course of action, the proposed control scheme achieved the desirable performance.

The next chapter explores prescribed-time adaptive neural consensus for uncertain nonlinear multi-agent systems. The goal is to achieve consensus among agents within a specified time frame using adaptive neural control techniques.